Eur. Phys. J. B **10**, 481–485 (1999)

THE EUROPEAN PHYSICAL JOURNAL B

EDP Sciences

A phenomenological model of percolating magnetic nanostructures

S.K. Wong[1], B. Zhao[1], T.K. Ng[1], X.N. Jing[1,a], X. Yan[1], and P.M. Hui[2,b]

[1] Department of Physics, Hong Kong University of Science and Technology, Clear Water Bay, Kowlon, Hong Kong
[2] Department of Physics, Chinese University of Hong Kong, Shatin, New Territories, Hong Kong

Received 4 November 1998

Abstract. Transport and magnetotransport properties were analysed systematically in percolating magnetic nanostructures such as Ni-rich NiFe−SiO_2 and Fe−SiO_2 films. These granular magnetic films exhibit giant Hall effect. We identified features which are common and unique to these systems. Among the features are the correlation between a $-\log(T)$-like temperature dependent resistivity and a particle size distribution having a large fraction of small nanometer sized particles, and the power law dependence between the magnetoresistivity and the room temperature resistivity. Assuming the presence of nanometer sized particles in the percolating conduction channels whose contributions are sensitive to temperature and the external magnetic field, we developed a phenomenological model to explain all the common features.

PACS. 85.70.Kh Magnetic thin film devices: magnetic heads (magnetoresistive, inductive, etc.); domain-motion devices, etc. – 72.15.Gd Galvanomagnetic and other magnetotransport effects – 75.60.-d Domain effects, magnetization curves, and hysteresis

1 Introduction

Spin-dependent transport phenomena have attracted much attention since the discovery of giant magnetoresistance (GMR) in metallic multilayers like Fe/Cr or Co/Cu [1–4]. It is widely believed that the GMR in such conducting systems are results of spin-dependent scattering from magnetically heterogeneous regions where local magnetizations are antiferromagnetically arranged [5,6]. Observation of GMR in immiscible magnetic granular composite films with a metallic matrix, such as Fe–Ag or Co–Ag [7,8], and those with an insulating matrix, such as Co–Al_2O_3 [9], indicate that spin-dependent scattering or tunnelling [10] is generic in all inhomogeneous magnetic nanostructures.

Ferromagnetic granular films in which giant Hall effect (GHE) was recently observed provide a new magnetic nanostructure to study spin-dependent transports with magnetic particles forming percolation conducting channels. GHE refers to a 10^4-fold enhancement in Hall resistivity in ferromagnetic granular $(NiFe)_x-(SiO_2)_{1-x}$ films for x near x_c, the percolation metal volume fraction [11], compared to that of a homogeneous ferromagnetic metal. The effect cannot be explained *via* a simple percolation theory that predicts a maximum enhancement factor of ~ 20 [12] based on the percolation critical exponent for Hall resistivity $g \sim 0.4$ [13] for a 1 μm thick film. Various attempts have been made to explain the giant Hall effect [14–17] but they so far have been unsuccessful. In fact, a complete microscopic theory for the GHE seems to be beyond our reach at the present moment since even the understanding of the extraordinary Hall effect in homogeneous transition metals is very limited [18,19]. The percolating labyrinth structure [20,12] in granular films adds further complication to the problem. Despite the complexity, the recently studied granular Fe–SiO_2 films [21] seems to indicate that there exist *unique* and *universal* features associated with a new conduction mechanism and spin dependent transports in magnetic metal-insulator nanocomposite films exhibiting giant Hall effect. In this paper, a systematic comparison of transport and magnetotransport properties in both $(NiFe)_x-(SiO_2)_{1-x}$ and $Fe_x-(SiO_2)_{1-x}$ films are carried out in which features common to the two percolating magnetic nanostructures closed to the percolation volume fraction, *i.e.*, $x \to x_c$, are presented. All the experimental data reported in this paper have been published in one form or another in references [11,12,14,15] by some of the present authors and coworkers. Motivated by the experimental features together with the observed size distribution of small particles in these samples [12], a phenomenological model is developed which captures the essence of these common features and which, we believe, also provides insights into the origin of the GHE.

The plan of the paper is as follows. In Section 2, we identify and examine the implications of the common and unique features in percolating magnetic granular films

[a] On leave from Institute of Physics, Chinese Academy of Sciences, Beijing, P.R. China.
[b] e-mail: pmhui@phy.cuhk.edu.hk

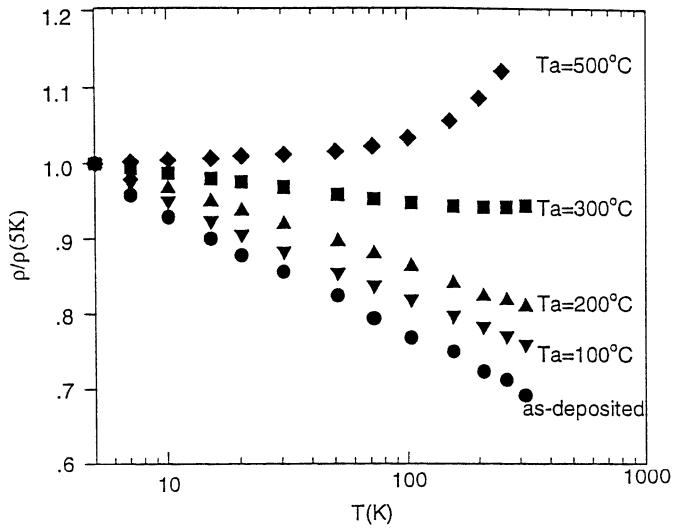

Fig. 1. Resistivity as a function of temperature for $Fe_{0.53}-(SiO_2)_{0.47}$ for various annealing conditions.

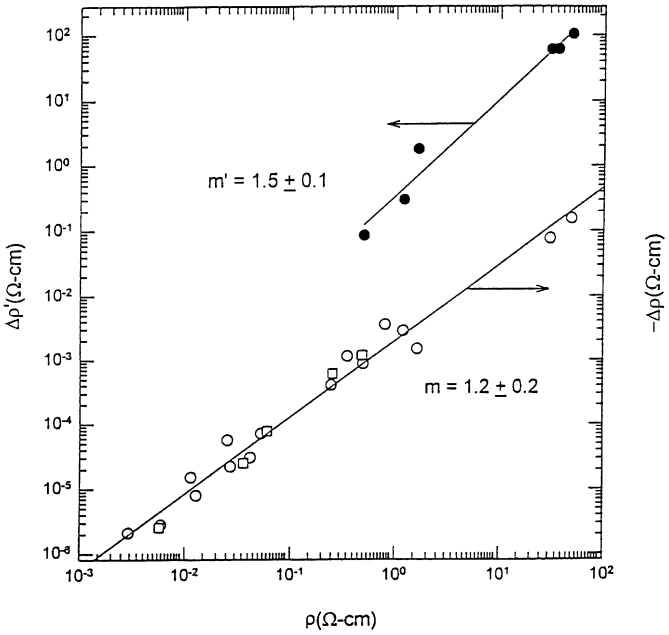

Fig. 2. Magnetoresistivity, $-\Delta\rho$, as functions of resistivity, ρ, in a log-log plot for NiFe$-SiO_2$ (open circle) and Fe$-SiO_2$ (open square), and temperature dependent part of resistivity, $\Delta\rho'$, *versus* ρ for NiFe$-SiO_2$ (filled circle).

exhibiting GHE. Our phenomenological model is introduced in Section 3 with results discussed and compared with observed experimental features. Our findings are summarized in Section 4

2 Characteristic features

In a series of experiments on GHE, Yan *et al.* [11,12,14,15,20–22] studied in detail the physical properties of granular magnetic films. It was discovered that for *all* samples studied so far exhibiting the giant Hall effect, including both NiFe–SiO_2 and Fe–SiO_2 films which have Hall coefficients of different signs [21] (positive(negative) for NiFe–SiO_2(Fe–SiO_2)), there always exists a large resistivity with a $\rho(T) \sim -\log(T)$-like temperature dependence. The resistivity reduces and the $\log(T)$-like behaviour goes away for samples annealed at high temperature, together with the disappearance of giant Hall effect. Figure 1 shows the temperature dependence of the resistivity (normalized to the value at 5 K) on a logarithmic scale for $Fe_{0.53}$–$(SiO_2)_{0.47}$ under different annealing temperatures T_a. For annealing below 300 °C, under which giant Hall effect exists (extraordinary Hall resistivity $\rho_{xys} \sim 0.1$ mΩcm, $\rho \sim 0.1$ Ωcm), the temperature dependent resistivity shows clearly a $\sim \log(T)$-like dependence. Whereas, for annealing above 300 °C, under which giant Hall effect disappears ($\rho_{xys} \sim 0.001$ mΩcm), the temperature dependence becomes metallic with considerably lower resistivity ($\rho \sim 0.1$ mΩcm). The same qualitative features were also found in NiFe–SiO_2 films [12].

We have also studied the magnetoresistivity of samples exhibiting giant Hall effect with magnetic field in the plane of the film both along and perpendicular to the current direction [22]. All geometries yield about the same negative value for the magnetoresistivity in films near the percolation threshold, both for NiFe–SiO_2 and Fe–SiO_2 systems, indicating that the magnetoresistance is a result of spin-dependent transport processes similar to many inhomogeneous magnetic nanostructures in which giant magnetoresistance were observed [1–9]. To investigate further the transport mechanism of the magnetoresistance in the region of giant Hall effect, we study the change in magnetoresistivity as a function of metal volume fraction in the range 52−65% for the as-deposited films. The results are plotted in Figure 2 in which we show the magnetoresistivity $-\Delta\rho$ *versus* resistivity on a log-log scale for Ni-rich NiFe–SiO_2 (circle) and Fe–SiO_2 (square) samples measured at 300 K. Note that the values of $-\Delta\rho$ in Fe–SiO_2 were divided by 4 to take into account the difference in the saturation magnetization because $-\Delta\rho$ scales with M^2 for a spin-dependent process. The solid line in the figure is the fitting according to $-\Delta\rho \sim \rho^b$, with $b \sim 1.2$. Note that scaling relationship between directly measurable physical variables such as resistivity and magnetoresistivity is much more reliable than scaling with $(x - x_c)$, since the former is insensitive to the determinations of both the metallic volume fraction x and its critical value x_c separating the metallic and insulating phases. It is clear from Figure 2 that within experimental error the *same power law* is found for both systems, suggesting that the same spin-dependent transport mechanism is functioning in both systems exhibiting the giant Hall effect, irrespective of the sign of the carriers and the details of the microstructures.

3 Phenomenological model

We propose that the universal behaviour associated with GHE observed in the two systems with very different

microscopic characters are results of their common percolating, granular structure. Our physical picture is based on the TEM observation that even in the metallic phase, well defined metallic clusters percolating throughout the whole sample are absent [12]. Instead, the conducting channels appear to be composed of metallic granular particles with a wide distribution in size [12]. The average distance between metallic grains decreases as the metal volume fraction increases. It thus appears that the conduction mechanism in these percolating nanostructures *cannot* be described by conventional classical percolation model. Instead, quantum tunneling between particles at close distances is the dominant mechanism of conduction. At zero temperature these systems should be described by quantum percolation models. However, at temperatures high enough so that the phase coherence between different tunneling events are lost, we may consider the system as a collection of classical resistors, but with possibly a wide distribution of resistances. Each metallic grain (resistor) is like a quantum dot with a given size and its behaviour has to be considered quantum mechanically when the size of the grain is small. To understand the transport behaviour of a collection of these particles we first consider a small metallic particle of size s^3 in a percolating conducting channel and study the problem of under what condition the particle can be considered as conducting. In general a metallic particle can be considered as conducting if there is no energy barrier against transporting electrons in and out of the particle. This is the case if the thermal energy $\sim k_{\rm B}T$ of electrons is larger than the energy level spacing inside the particle, $\Delta E(s) \sim \frac{\hbar^2}{2m^* s^2}$, where m^* is the electron effective mass, or $\Delta E(s) \sim \frac{e^2}{\epsilon s}$, where ϵ is the effective dielectric constant, if Coulomb blockade effect is important [23]. In our granular systems in which a large number of small particles with dimension $s \leq 3$ nm exist [12], it is expected that this finite size effect will be important. The small particles which behave as metals at high temperature, would become insulating at temperature $k_{\rm B}T \leq \Delta E(s)$, leading to an increasing resistance at low temperature. The behaviour of the system can be described by a *continuum* percolation model, in which the conducting network is formed by (classical) resistors with a wide distribution of resistances [24–26]. The distribution of resistance depends on the size distribution of metallic particles, as well as on temperature. In the case when the particles are magnetized and with magnetization pointing in random directions, which is believed to be the case in the absence of a strong magnetic field aligning the magnetizations, there are additional energy barriers between particles with magnetization pointing in different directions [28]. These energy barriers are highest when the magnetization of the particles are pointing in opposite directions [28]. These energy barriers are lowered when a large magnetic field is applied on the system, since the magnetization of the particles will be aligned *on average*, leading to decrease in resistances and negative magnetoresistance.

While the actual distribution in resistances is difficult to determine in a sample, it is possible to construct a phenomenological model which captures the essence of the physical picture discussed above. To capture these effects at least qualitatively, we assume that the transport properties of the magnetic granular systems under consideration can be described by a continuum percolation model near percolation threshold in which the resistivity is given by the formula

$$\rho(T,H) = \frac{\rho_0}{(x_{\rm eff}(T,H) - x_{\rm c})^t}, \tag{1}$$

where ρ_0 is a material dependent parameter, t is a critical exponent [13] characterizing the resistivity, $x_{\rm eff}(T,H)$ is the effective conducting volume fraction, and H is the external magnetic field. In classical percolation problems in three dimensions, the t-exponent is universal and takes on the value $t \sim 2.0$ [27]. It is, however, well known that in continuum percolation, the critical exponent t is no longer universal but with its precise value depending on the form of the distribution in resistances among the resistors [24,25]. Here, the exponent t is simply taken as a parameter [11] in our phenomenological model. For the effective volume fraction, we expect from our previous discussion that at zero external magnetic field,

$$x_{\rm eff}(T,0) \sim \int_{s(T)}^{\infty} (s^3) n(s) {\rm d}s = x_0 - \int_0^{s(T)} (s^3) n(s) {\rm d}s, \tag{2}$$

where $n(s){\rm d}s$ is the number of particles in the sample with linear dimension between s and $s+{\rm d}s$, $x_0 = \int_0^{\infty} (s^3) n(s) {\rm d}s$ is the metal volume fraction, which was determined by EDX. The cutoff linear dimension $s(T)$ is determined by the equation $k_{\rm B}T = \Delta E(s)$, and only particles with dimension larger than $s(T)$ contribute to conduction. At finite magnetic field, we expect that $x_{\rm eff}$ increases because of alignment of magnetization among different particles on average. The precise magnetic field dependence of this effect is hard to estimate. However, at $H > H_{\rm s}$ where $H_{\rm s}$ is the saturation magnetization field, the magnetic field dependence of $x_{\rm eff}$ should become weak. Therefore, we expect

$$x_{\rm eff}(T, H > H_{\rm s}) \sim x_{\rm eff}(T,0) + \Delta x_{\rm M}(T), \tag{3}$$

where $\Delta x_{\rm M}(T) \sim A \int_{s(T)}^{\infty} (\lambda)(s^2) n(s) {\rm d}s$ with A being a constant depending on the microscopic details of the material. The integral $\int_{s(T)}^{\infty} (\lambda)(s^2) n(s) {\rm d}s$ measures the average geometrical volume occupied by magnetic domain walls between different grains where $\lambda \sim$ thickness of the domain wall [28]. For samples where no measurable saturation field $H_{\rm s}$ exists, a more microscopic model is needed to describe $\Delta x_{\rm M}(T,H)$ and is beyond the scope of our simple phenomenology.

Substituting equation (2) into equation (1), and assuming that the change in $x_{\rm eff}$ is small, we obtain at zero magnetic field,

$$\rho(T,0) \sim \rho_{\infty} \left(1 + t(\frac{\rho_{\infty}}{\rho_0})^{1/t} \int_0^{s(T)} (s^3) n(s) {\rm d}s \right), \tag{4}$$

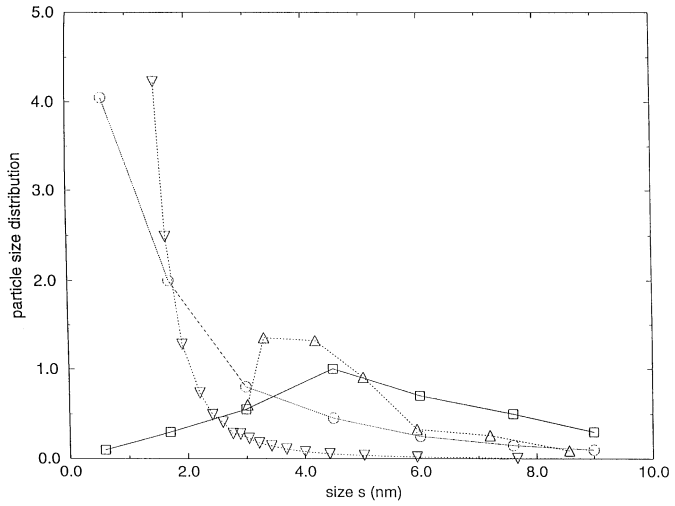

Fig. 3. Particle size distributions ($\times 10^{11}/\mathrm{mm}^2$) determined by TEM (solid line) and from equation (5) using temperature dependent resistivity data (dash-line) for (a) $Ni_{0.55}-(SiO_2)_{0.45}$ as deposited (◯ (TEM), ∇ (theory)), and (b) $Ni_{0.55}-(SiO_2)_{0.45}$ annealed at 520 °C (□ (TEM), △ (theory)).

where $\rho_\infty = \rho_0/(x_0 - x_c)^t$ is the high temperature resistivity. It follows that

$$\frac{\mathrm{d}\rho(T,0)}{\mathrm{d}T} = t\rho_\infty \left(\frac{\rho_\infty}{\rho_0}\right)^{1/t} \frac{\mathrm{d}s(T)}{\mathrm{d}T}(s(T))^3 n(s(T)), \qquad (5)$$

which provides a precise relation between $\mathrm{d}\rho(T,0)/\mathrm{d}T$ and particle size distribution $n(s(T))$ which can be tested experimentally. In particular, in the temperature range where $\rho(T,0) \sim -\log(T)$, we find correspondingly $n(s) \sim s^{-4}$. Notice that this behaviour is independent of the origin of $\Delta E(s)$ and remains the same as long as $\Delta E(s) \sim s^{-a}$, with $a \geq 1$. Rapid increase in $n(s)$ as s decreases was indeed observed experimentally [12] for samples with $\rho(T) \sim -\log(T)$. Note that the $n(s) \sim s^{-4}$ behaviour disappears at small enough s, as can be seen from magnetoresistance data in which the $\rho \sim -\log(T)$ behaviour vanishes at high enough temperature. For annealed samples in which the $\rho(T) \sim -\log(T)$ behaviour is absent, it was also observed that the rapid increase in $n(s)$ at small s is destroyed and the peak in $n(s)$ was gradually shifted to higher values of s when annealing temperature is increased [12]. The same qualitative behaviour was also obtained from equation (5) using the experimental data for $\rho(T,0)$ as input. Figure 3 shows the particle size distribution $n(s)$ for $(NiFe)_x$–$(SiO_2)_{1-x}$ as deposited films and films annealed at 520 °C. The experimental data are obtained by TEM measurements and reproduced from reference [12], whereas the theoretical results are the size distribution derived from equation (5) using the corresponding resistivity data as input with $\Delta E(s) = \frac{\hbar^2}{2ms^2}$, where m is the free electron mass. The qualitative, and to a certain extent quantitative, agreement between theory and experiment is apparent. Fitting with $\Delta E(s) = e^2/\epsilon s$ to experimental data was also tried but the agreement with experimental data is slightly worse. It should be stressed that the agreement between theory and experiment indicates that the phenomenological model captures the essential physics of the systems. However, it must be cautioned that so far the available experimental data and the theory are both too crude to determine precisely the origin of $\Delta E(s)$ in our systems.

Our phenomenological model also predicts a scaling relationship between the magnetoresistivity and the resistivity. Using equations (1) and (3), it is easy to show that the saturated magnetoresistivity $\Delta\rho$ is given by

$$\Delta\rho = -t\rho_\infty \left(\frac{\rho_\infty}{\rho_0}\right)^{1/t} \Delta x_{\mathrm{M}}(T). \qquad (6)$$

Using 300 K as the high temperature limit, we obtain $\Delta\rho \sim (\rho_\infty)^b \sim \rho^b$ near the percolation threshold, where $b = 1 + t^{-1}$, which, within experimental accuracy, is consistent with experimental values of $b \sim 1.2 \pm 0.1$ and $t \sim 3.6 \pm 1.0$ [11]. From equation (4), our phenomenological theory also predicts that the temperature dependent part of the resistivity at $H = 0$ should also scale similarly as $\Delta\rho$, *i.e.* $\Delta\rho' \equiv \rho(T,0) - \rho_\infty \sim (\rho_\infty)^{1+t^{-1}}$. Taking $T = 77$ K, we also show in Figure 2 the temperature dependent part of resistivity $\Delta\rho'$ *versus* resistivity ρ (300 K) on a log-log scale for $(NiFe)_x$–$(SiO_2)_{1-x}$ samples (filled circles). Here only samples with $\rho \sim 0.4$ Ωcm or above were considered since samples with lower resistivity have minimum in the temperature dependence. The similar scaling behaviour of $\Delta\rho$ and $\Delta\rho'$ *versus* ρ is apparent from the figure, as predicted by our simple model.

It should be emphasized that the temperature dependence of resistivity and magnetoresistance are usually results of very different physical processes and it is highly unusual that they both scale with resistivity with a similar critical exponent. The observed qualitative agreement in the critical exponents of the two resistivities, thus, strongly supports our physical picture that the temperature and magnetic field dependent effective conduction volume fraction dominates the physics of percolating magnetic nanostructures.

Our phenomenology in describing the dependence of resistivity on the temperature, the magnetic field, and the particle size distribution, in various percolating magnetic nanostructures, is reasonably successful. This leads us to the question of whether similar phenomenology can be applied to describe the Hall resistances, and in particular, whether the physical origin of the GHE can be identified from our phenomenology. Following our previous analysis, we propose that the Hall resistivity can be described by the formula

$$\rho_{xy}(T,H) = \frac{BR_0}{(x_{\mathrm{eff}}(T,H) - x_c)^g}, \qquad (7)$$

where R_0 is a material dependent parameter and $B = H + 4\pi M$ is the total magnetic field on the electrons in the system. The Hall number $R_{\mathrm{H}} \sim \rho_{xy}/H \sim (x_{\mathrm{eff}}(T,H) - x_c)^{-g}$ and extraordinary resistivity $\rho_{xys} \sim M/(x_{\mathrm{eff}}(T,H) - x_c)^g$ are predicted to scale with $\rho(T,H)$ with the same exponent ($R_{\mathrm{H}}(\rho_{xys}) \sim \rho^{g/t}$) near the percolation threshold

in our phenomenology, which is consistent with existing data where $g/t \sim 0.8$ within experimental accuracy [29].

Perhaps the most surprising result in our phenomenological model is that the values of exponents $t \sim 3.6$ and $g \sim 2.9$ deduced experimentally [11] are large compared with the corresponding values $t \sim 2.0$ and $g \sim 0.4$ obtained in the usual classical percolation models [13,27]. In particular, the large enhancement of the critical exponent g (a factor of 7 over the theoretical value of 0.4) is responsible for the large magnitude of Hall resistance observed near the percolation threshold, whereas the relatively smaller enhancement in t (by a factor of 1.8) seems to be the reason why the enhancement in magnetoresistance is not as drastic as the Hall effect. It should be pointed out that similar enhancement in the t-exponent has been previously observed in experiments on continuum peroclating systems using silver-coated-glass–Teflon random composites [30]. The experimentally observed large t-exponent is hence consistent with the continuum percolation picture employed in the present model. The key to understand the giant Hall effect seems to lie in the problem of understanding the physical origin of these unusually large values of critical exponents. Within the continuum peroclation picture, the enhancement in the exponents over their classical values arises from a wide distribution of resistances. This distribution, in turn, is sensitive to the size distribution of grains, the metal volume fraction, temperature, and magnetic field in ferromagnetic granular films.

4 Summary

In summary, we have identified a few unique correlated features in transport properties in percolating magnetic nanostructures exhibiting giant Hall effect. These features include the correlation between a $-\log(T)$-like temperature dependent resistivity and a particle size distribution having a large fraction of small nanometer sized particles, the power law dependence between the magnetoresistivity and the room temperature resistivity, and that of the temperature dependent part of resistivity and room temperature resistivity. These unique features are explained within a phenomenological model developed in this work, assuming the presence of nanometer sized particles in the percolating conducting channels, whose contribution to the conduction is sensitive to temperature and the external magnetic field. Note that similar ideas have been employed to explain the temperature and bias-voltage dependence of the magnetoresistance in percolating magnetic nanostructures in the insulating side [31]. We believe that the key to understand the origin of the giant Hall effect lies in the understanding of the unusually large critical exponents.

The authors would like to acknowledge Yingfan Xu and Alec Pakhomov for important contributions in the early stage of the work, and Jie Xhie, Stephen Leung, Lu Tao Weng for sample preparation and characterizations, and Ping Sheng and Kwok Kung Fung for useful discussions. This work was supported by Research Grants Council (RGC) of the Hong Kong SAR Government under grant HKUST692/96P.

References

1. M.N. Baibich *et al.*, Phys. Rev. Lett. **61**, 2472 (1988).
2. G. Binasch, P. Grunberg, F. Saurenbach, W. Zinn, Phys. Rev. B **39**, 4828 (1989).
3. J.J. Kerbs, P. Lubitz, A. Chaiken, G.A. Prinz, Phys. Rev. Lett. **63**, 1645 (1989).
4. S.S.P. Parkin, N. More, K.P. Roche, Phys. Rev. Lett. **64**, 2304 (1990).
5. R.E. Camley, J. Barnas, Phys. Rev. Lett. **63**, 664 (1989).
6. P.M. Levy, S. Zhang, A. Fert, Phys. Rev. Lett. **65**, 1643 (1990).
7. A.E. Berkowitz *et al.*, Phys. Rev. Lett. **68**, 3745 (1992).
8. J.Q. Xiao, J.S. Jiang, C.L. Chien, Phys. Rev. Lett. **68**, 3749 (1992).
9. H. Fujimori, S. Mitani, S. Ohnuma, J. Magn. Magn. Mater. **156**, 311 (1996).
10. J.I. Gittleman, Y. Goldstein, Bozowski, Phys. Rev. B **5**, 3609 (1972); B. Abeles, P. Sheng, M.D. Couts, Y. Arie, Adv. Phys. **24**, 407 (1975); B. Abeles, H.L. Pinch, J.I. Gittleman, Phys. Rev. Lett. **35**, 247 (1975).
11. A.B. Pakhomov, X. Yan, B. Zhao, Appl. Phys. Lett. **67**, 3497 (1995).
12. X.N. Jing *et al.*, Phys. Rev. B **53**, 14023 (1996).
13. D.J. Bergman, D. Stroud, in Solid State Physics, *Advances in Research and Applications*, edited by H. Ehrenreich, D. Turnbull (Academic, New York, 1992), Vol. 46, p. 147.
14. A.B. Pakhomov, X. Yan, Solid State Commun. **99**, 139 (1996).
15. A.B. Pakhomov, X. Yan, Y. Xu, J. Appl. Phys. **79**, 6140 (1996).
16. F. Brouers, A. Granovsky, A. Sarychev, A. Kalitsov, Physica A **241**, 284 (1997).
17. P. Sheng (private communication).
18. P. Nozières, C. Lewiner, J. Phys. France **34**, 901 (1973).
19. L. Berger, Phys. Rev. B **2**, 4559 (1970).
20. Y. Xu, B. Zhao, X. Yan, J. Appl. Phys. **79**, 6137 (1996); Y. Xu, X. Yan, J. Mater. Res. **11**, 2506 (1996).
21. B. Zhao, X. Yan, J. Appl. Phys. **81**, 4290 (1997).
22. B. Zhao, X. Yan, A.B. Pakhomov, J. Appl. Phys. **81**, 5527 (1997).
23. Y. Meir, N.S. Wingreen, P.A. Lee, Phys. Rev. Lett. **66**, 3048 (1991).
24. P.M. Kogut, J.P. Straley, J. Phys. C **12**, 2151 (1979); J.P. Straley, J. Phys. C **15**, 2343 (1982).
25. B.I. Halperin, S. Feng, P.N. Sen, Phys. Rev. Lett. **54**, 2391 (1985); S. Feng, B.I. Halperin, P.N. Sen, Phys. Rev. B **35**, 197 (1987).
26. P.M. Hui, D. Stroud, Phys. Rev. B **32**, 7728 (1985).
27. H.J. Herrmann, B. Derrida, J. Vannimenus, Phys. Rev. B **30**, 4080 (1994).
28. M. Yamanaka, N. Nagaosa, J. Phys. Soc. Jap. **65**, 3088 (1996); see also G. Tatara, H. Fukuyama, Phys. Rev. Lett. **78**, 3773 (1997).
29. A.B. Pakhomov *et al.*, Physica A **241**, 344 (1997).
30. S.I. Lee, Y. Song, T.W. Noh, X.-D. Chen, J.R. Gaines, Phys. Rev. B **34**, 6719 (1986).
31. S. Mitani *et al.*, Phys. Rev. Lett. **81**, 2799 (1998); see also J. Inoue, S. Maekawa, Phys. Rev. B **53**, 11927 (1996).